www.czasopisma.pan.pl PAN www.journals.pan.pl

ARCHIVES of FOUNDRY ENGINEERING

ISSN (2299-2944)
Volume 2020
Issue 4/2020

145 – 153

10.24425/afe.2020.136069

21/4

Published quarterly as the organ of the Foundry Commission of the Polish Academy of Sciences

Analysis of the Microstructure, Properties and Machinability of Al-Cu-Si Alloys

J. Kozana, M. Piękoś, M. Maj, A. Garbacz-Klempka*, P.L. Żak
AGH University of Science and Technology, Faculty of Foundry Engineering,
Reymonta 23 Str., 30-059 Kraków, Poland
* Corresponding author. E-mail address: agarbacz@agh.edu.pl

Received 22.12.2020; accepted in revised form 29.12.2020

Abstract

As part of the studies conducted in the field of broadly understood casting of non-ferrous metals, selected results on the impact of variable additions of copper and silicon in aluminium were presented. A series of melts was carried out with copper content kept constant at a level of 2% (1st stage) and 4% (2nd stage) and variable contents of silicon introduced into aluminium. The crystallization characteristics of the examined alloys and the percentage of structural constituents at ambient temperature were obtained by modelling the thermodynamic parameters of individual phases with the CALPHAD method. The microstructure of the obtained alloys was examined and microhardness was measured by the Vickers-Hanemann method. The alloy properties were assessed based on the results of mechanical tests, including ultimate tensile strength (UTS), hardness (BHN) and elongation (E). The machinability of the tested alloys was analyzed in a machinability test carried out by the Keep-Bauer method, which consisted in drilling with a constant feed force.
The obtained results clearly indicate changes in the images of microstructure, such as the reduction in grain size, solution hardening and precipitation hardening. The changes in the microstructure are also reflected in the results of mechanical properties testing, causing an increase in strength and hardness, and plasticity variations in the range of 4 ÷ 16%, mainly due to the introduced additions of copper and silicon. The process of alloy strengthening is also visible in the results of machinability tests. The plotted curves showing the depth of the hole as a function of time and the images of chips produced during the test indicate an improvement in the wear resistance obtained for the tested group of aluminium alloys with the additions of copper and silicon.

Keywords: Casting, Aluminum Alloys, Ternary Al-Cu-Si alloy, Mechanical Properties, Microstructure, Thermo-Calc

1. Introduction

Non-ferrous metals and alloys play a very important role in technology and it would be difficult to imagine the development of this technology without the contribution of modern casting materials based on non-ferrous metals. The continuous progress of science and technology has resulted in the introduction to the market of a large number of non-ferrous alloys with very diverse compositions and properties, used mainly in such areas as electrical engineering, and automotive, aviation, rocket, transport and construction industries. In practice, aluminium alloys are most often used. Owing to the introduction of alloying elements, they are characterized by very good mechanical properties [1], combined with excellent castability, low density and good corrosion resistance [2-5].

Efforts are continuously made to improve their usability thanks to such procedures as the selection and optimization of chemical composition, refining and modification processes, the selection of casting technology and heat treatment parameters [6-14]. All these treatments allow obtaining materials with very good mechanical properties, high placticity, and satisfactory hardness,which in turn gives products characterized by good,

resistance to the effect of high temperature and corrosive environment. Aluminium-silicon alloys are widely used in the automotive industry [15-18], aviation [19-26]. Copper controls the strength and hardness of casting aluminium alloys. Aluminium alloys, including AlCu alloys, are the subject of studies of the effect of additives on the nucleation process and crystal growth [27-28]. Ternary alloys from the Al-Cu-Si system are gaining more and more popularity. They are lightweight and superior to Al-Si alloys in terms of strength and to Al-Cu alloys in terms of corrosion resistance. These features explain the growing interest in Al-Cu-Si alloys in the automotive and aviation industries [29-32].

2. Materials and Methods

The aim of this study was to analyze the influence of the variable content of silicon additions on the properties of an Al - Cu alloy. In alloys made of pure components, special attention was paid to the mechanical properties of samples cast into metal moulds. Chemical and microstructural analyses were performed during the tests, and properties such as ultimate tensile strength (UTS), elongation (E) and machinability were determined. Hardness (HBN) was measured by the Brinell method and microhardness (μHV) by the Vickers-Hanemann method.

In the first stage of research work, it was planned to prepare the melts and produce samples of Al alloys with a constant copper content of 2% and variable silicon contents, introduced into aluminium in the amounts of 0.5%, 1.5%, 3%. In the second stage, the constant copper content was 4%, while silicon was introduced in the amounts of 0.1%, 2% and 4% (Table 1)

Table 1.
Plan of the experiment with varied content of alloying elements in aluminium

Average content of alloying elements (wt%)					
Stage No. 1			**Stage No. 2**		
No.	Cu	Si	No.	Cu	Si
1.1	2.0	0.5	2.1	4.0	0.1
1.2	2.0	1.5	2.2	4.0	2.0
1.3	2.0	3.0	2.3	4.0	4.0

The equilibrium crystallization analysis was carried out by the CALPHAD (CALculation of PHAse Diagrams) method using a Thermo-Calc package with the TCS Al-based Alloys Database [40-42].

Melts were prepared in a pilot foundry of the AGH Faculty of Foundry Engineering. A medium frequency induction furnace was used for metal melting. The charge was melted in a chamotte-graphite crucible. The following charge materials were used: electrolytic aluminium A199.99 (designated as AR1) according to PN-EN 1676:2020-09, crystalline silicon and cathode electrolytic copper in the form of plates with the minimum copper content of 99.99% according to PN-EN 1982:2017-10.

As part of preliminary tests, the primary AlCu50 alloy was prepared. During casting, the pouring temperature was controlled and kept in the range of 730–750ºC, the metal mould temperature was 150–170ºC.

The quality of the performed melts was checked by the analysis of chemical composition. For this purpose, a SPECTROMAXx emission spectrometer was used. The results of the analysis are presented in Table 2. They confirm that melting was carried out in a proper way, since the obtained samples of AlCuSi alloys contain only small amounts of impurities, mainly iron and zinc.

Table 2.
The results of the chemical analysis of the tested samples

The content of elements in the alloy (wt%)					
Stage No. 1					
No.	Cu	Si	Fe	Zn	Al
1.1	2.04	0.075	0.014	0.024	bal.
1.2	2.06	1.58	0.019	0.075	bal.
1.3	2.27	2.87	0.034	0.069	bal.
Stage No. 2					
No.	Cu	Si	Fe	Zn	Al
2.1	4.29	0.088	0.019	0.024	bal.
2.2	4.26	1.80	0.032	0.016	bal.
2.3	4.17	3.92	0.029	0.032	bal.

Microstructure was examined by the light microscopy (LM) using an Eclipse LV 150 microscope. The microhardness (μHV) of structural phases was tested by the Vickers-Hanemann method. The ultimate tensile strength (UTS) and the elongation (E) of the alloys were assessed on an INSTRON device, model 1115.

Hardness was measured by the Brinell method (BHN). The assessment of machinability was done by the Keep-Bauer method measuring the cutting force. The machinability test consisted in drilling a 6 mm diameter hole in the prepared samples using drill [43].

3. Results and Discussion

3.1. Thermodynamic predictions

Modelling of alloys by the CALPHAD method was carried out for the experimental chemical composition shown in Table 2, using a Thermo-Calc software. The program analyzes the three main elements, i.e. Al, Cu and Si, and also elements such as zinc and iron, present in the alloy and treated as impurities. The alloy cooling process was simulated allowing for the phase transformations under equilibrium conditions.

As a result of modelling, graphs of theoretical crystallization were plotted for the examined alloys. The graphs show the effect of individual elements on the crystallization characteristics of individual phases. A sample simulation graph of the AlCuSi alloy cooling process is shown in Figures 1-4.

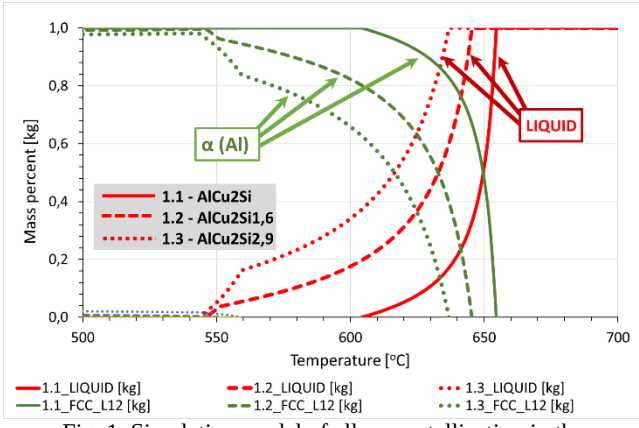

Fig. 1. Simulation model of alloy crystallization in the temperature range 700-500 ° C, determined for alloys 1.1-1.3.

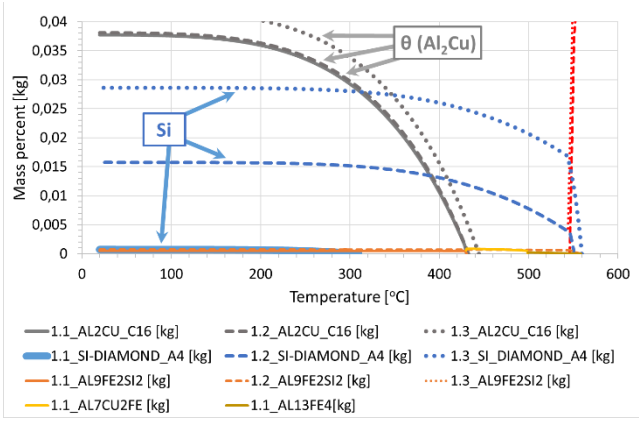

Fig. 2. Simulation model of alloy crystallization in the temperature range 600-200 °C (fragment of the graph of the phase content 0-0.04 % m/m), determined for alloys 1.1-1.3.

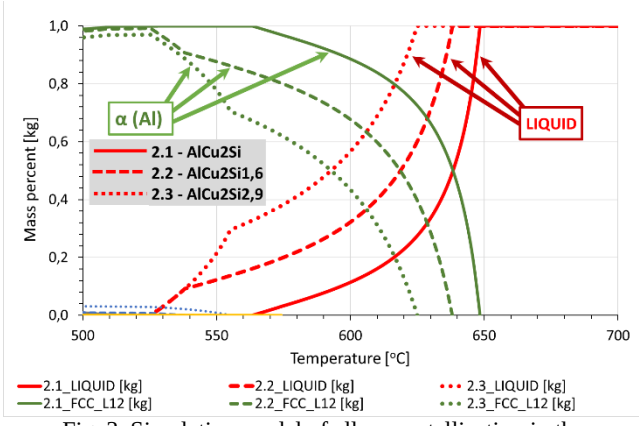

Fig. 3. Simulation model of alloy crystallization in the temperature range 700-500 ° C, determined for alloys 2.1-2.3.

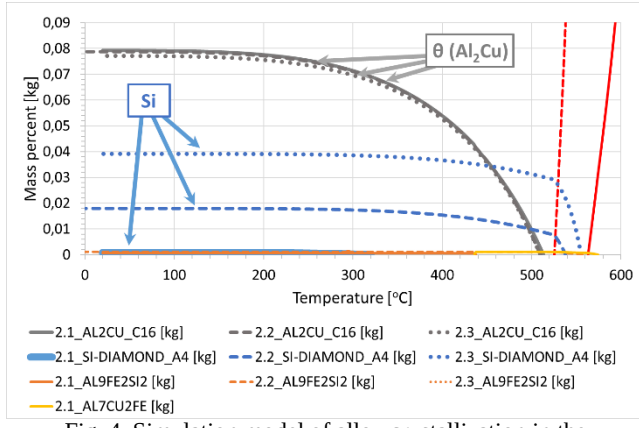

Fig. 4. Simulation model of alloy crystallization in the temperature range 600-200 °C (fragment of the graph of the phase content 0-0.09 % m/m), determined for alloys 2.1-2.3.

In modelled cases of crystallization of the examined alloys, at a temperature of 20°C, four phases occur in the alloy structure and their proportional content depends on the chemical composition. The three phases are typical phases present in AlCu and AlCuSi alloys, i.e. FCC_L12 phase (green colour in the graphs and tables) - the α phase treated as aluminium, AL2CU_C16 phase (grey colour) - the intermetallic θ phase - Al_2Cu phase, and SI-DIAMOND_A4 phase (blue colour), which corresponds to the crystal structure of diamond (A4) and in this case is pure silicon. The fourth disclosed AL9FE2SI2 phase (brown colour) is a multi-component phase associated with the presence of Fe in the tested alloys containing Al, Fe and Si, respectively. A small amount of zinc revealed in the composition of the tested alloys is part of the FCC_L12 phase. The content of individual elements in the phases that occur during alloy crystallization is summarized in Table 3.

Table 3.
The content of individual elements in the phases occurring during crystallization of the examined AlCuSi alloys

Phase	Mass percent of element in phase				
	Al	Cu	Si	Zn	Fe
FCC_L12	99.9632	0.0005		0.0362	
AL2CU_C16	45.9233	54.0765	0.0001		
AL9FE2SI2	64.1126		8.9216		26.9657
SI-DIAMOND_A4			100.0000		

Tables 4 and 5 show the results of Thermo-Calc modelling of the tested AlCuSi alloys. The increasing content of copper and silicon additions directly affects the drop of the crystallization start temperature T_1 and the remaining temperatures T_2 - T_7 determined during modelling of the tested alloys crystallization process. Alloys 1.1 and 2.1 are AlCu alloys where the α phase (FCC_L12) and the precipitates of the Al_2Cu phase (AL2CU_C16) are observed to occur at ambient temperature. The presence of the remaining phases, i.e. SI-DIAMOND_A4 and AL9FE2SI2, results from the trace content of silicon and iron in the chemical composition of the alloy, determined by the Thermo-Calc program at a level of 0.05–0.07%.

Table 4.
The results of Thermo-Calc modelling of characteristic phase transformation temperatures in the tested AlCuSi alloys (1.1-1.3)

Sample	T_1[°C]	T_2[°C]	T_3[°C]	T_4[°C]	T_5[°C]	T_6[°C]	T_7[°C]	T_8[°C]	Mass fraction in 20°C
1.1 AlCu2SiFeZn									
LIQUID [kg]	654	606							
FCC_L12 [kg]	654	606				430		20	0.9610
AL2CU_C16 [kg]						430		20	0.0377
AL7CU2FE [kg]					498	430			
AL13FE4 [kg]			558		498				
AL9FE2SI2 [kg]						430		20	0.0005
SI-DIAMOND_A4 [kg]							309	20	0.0007
1.2 AlCu2Si1,6FeZn									
LIQUID [kg]	645		558	546					
FCC_L12 [kg]	645		558	546		432		20	0.9454
AL2CU_C16 [kg]						432		20	0.0380
AL9FE2SI2 [kg]			558					20	0.0007
SI-DIAMOND_A4 [kg]				550				20	0.0157
1.3 AlCu2,2Si2,9FeZn									
LIQUID [kg]	636		559	543					
FCC_L12 [kg]	636		559	543		444		20	0.9281
AL2CU_C16 [kg]						444		20	0.0419
AL9FE2SI2 [kg]			555					20	0.0013
SI-DIAMOND_A4 [kg]			559					20	0.0286

Table 5.
The results of Thermo-Calc modelling of characteristic phase transformation temperatures in the tested AlCuSi alloys (2.1-2.3)

Sample	T_1[°C]	T_2[°C]	T_3[°C]	T_4[°C]	T_5[°C]	T_6[°C]	T_7[°C]	T_8[°C]	Mass fraction in 20°C
2.1 AlCu4,3SiZnFe									
LIQUID [kg]	648		563						
FCC_L12 [kg]	648		563	513				20	0.9192
AL2CU_C16 [kg]				513				20	0.0793
AL7CU2FE [kg]			574			435			
AL9FE2SI2 [kg]						437		20	0.0007
SI-DIAMOND_A4 [kg]							319	20	0.0008
2.2 AlCu4,3Si1,8ZnFe									
LIQUID [kg]	638		538	525					
FCC_L12 [kg]	638		538	525	509			20	0.9021
AL2CU_C16 [kg]					509			20	0.0787
AL9FE2SI2 [kg]			556					20	0.0012
SI-DIAMOND_A4 [kg]			538					20	0.0179
2.3 AlCu4,2Si4ZnFe									
LIQUID [kg]	624		555	525					
FCC_L12 [kg]	624		555	525	509			20	0.8827
AL2CU_C16 [kg]					509			20	0.0771
AL9FE2SI2 [kg]			545					20	0.0011
SI-DIAMOND_A4 [kg]			555					20	0.0391

The Al_7Cu_2Fe and $Al_{13}Fe_4$ phases present during crystallization are unstable and do not occur at ambient temperature. In the temperature range of 550-559°C, the introduction of silicon in an amount exceeding 1.6% results in more silicon appearing in the form of the SI-DIAMOND_A4 phase, which at ambient temperature (20°C) reaches the percent content of an alloying constituent. The Al_2Cu phase crystallizes in the solid state and its crystallization temperature depends on the copper content (430-513°C). In all cases, at 20°C, the content of the $Al_9Fe_2Si_2$ phase is at a low level of 0.07 - 0.13%.

3.2. Microstructural characterization

In the next stage of the studies, the impact of the introduced variable additions of silicon and copper on changes in the images of the microstructure of the examined alloys was evaluated. A 10% aqueous NaOH solution was used for etching of the metallographic specimens. Figures 5-9 show microstructure of the examined alloys with different content of copper and silicon.

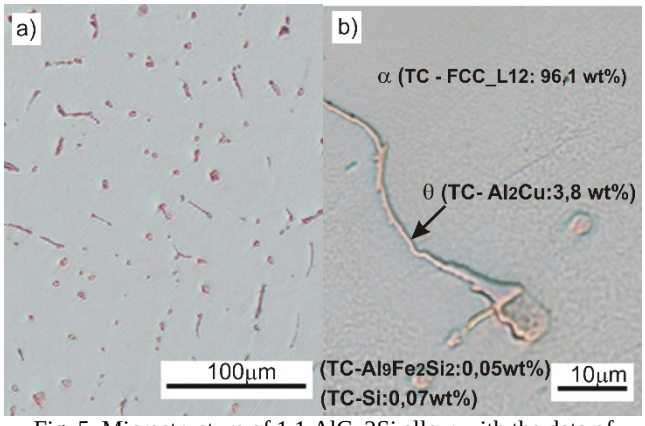

Fig. 5. Microstructure of 1.1 AlCu2Si alloy; with the data of Thermo-Calc; a) 100x; b) 500x

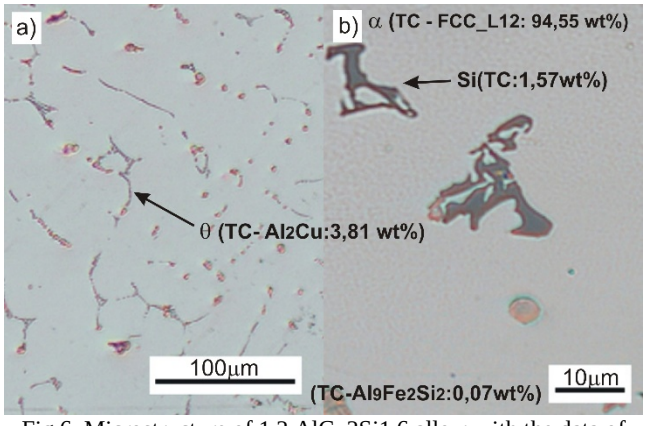

Fig.6. Microstructure of 1.2 AlCu2Si1,6 alloy; with the data of Thermo-Calc; a) 100x; b) 500x

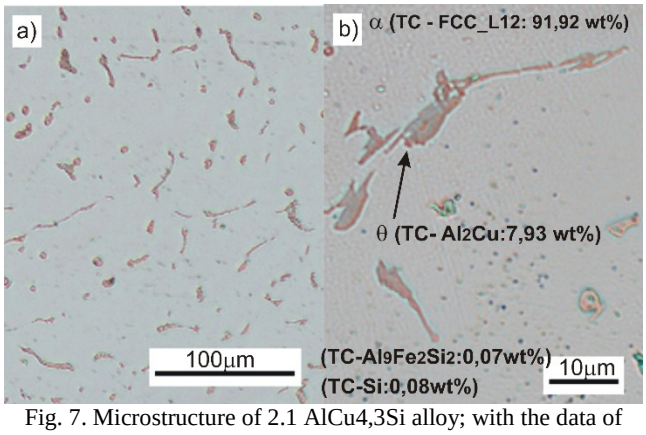

Fig. 7. Microstructure of 2.1 AlCu4,3Si alloy; with the data of Thermo-Calc; a) 100x; b) 500x

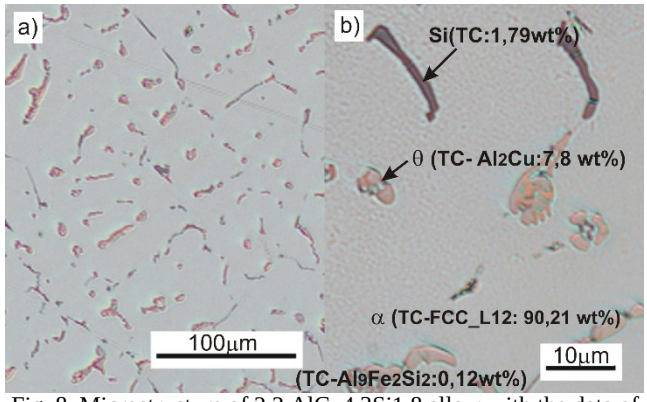

Fig. 8. Microstructure of 2.2 AlCu4,3Si1,8 alloy; with the data of Thermo-Calc; a) 100x; b) 500x

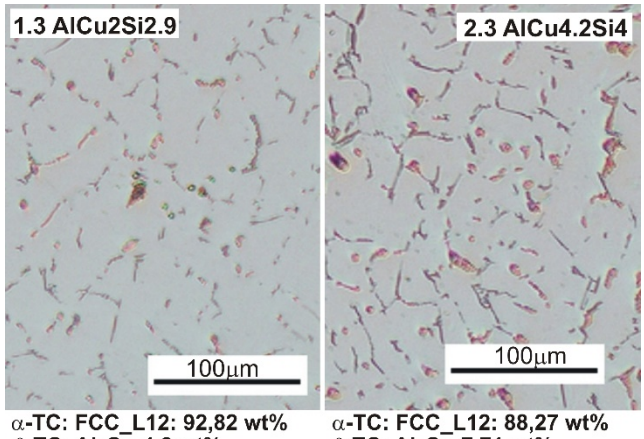

Fig. 9. Microstructure of 1.3 AlCu2Si2.9 and 2.3 AlCu4,2Si4 alloy; with the data of Thermo-Calc; 100x

The drawings show images of the microstructure of the tested samples with a variable copper content of 2% and 4%, and a variable addition of silicon. Based on the phase diagram of the Al-Cu-Si alloy, calculated by the Calphad method, it is possible to determine individual constituents revealed in the microstructure of the examined alloys. The images of microstructure show the contribution of individual phases at ambient temperature, modelled with the Thermo-Calc program.

In the images of microstructure, the dominant constituent is the solid solution of copper in α aluminium, accompanied by numerous precipitates of the Al_2Cu phase crystallites. With the increasing percent content of silicon, the presence of characteristic silicon crystallites in the form of large, irregular precipitates is also observed.

The precipitates of the Al_2Cu phase, occurring in the microstructure of the examined alloys, are characterized by a favourable dispersion distribution, which increases both hardness and strength. However, a very high proportional contribution of the Al_2Cu phase, present especially at the grain boundaries, can weaken the alloy and even prevent making a sound, crack-free casting.

3.3. Mechanical properties

A comparison of the results of the strength, hardness and microhardness testing is presented in Table 6 and graphically in Figure 10.

Table 6.
Mechanical properties of AlCuSi alloys

No.	UTS (MPa)	Elongation E (%)	Hardness HBN	Microhardness μHV
Stage No. 1				
1.1	94	9.31	37.8	53.5
1.2	117	16.54	47.8	55.7
1.3	133	10.98	55.2	64.8
Stage No. 2				
2.1	136	5.43	48.2	54
2.2	171	7.56	61.7	74.6
2.3	182	4.64	68.1	79.5

Analyzing the results of testing the tensile strength R_m of alloys with 2% and 4% Cu, it can be concluded that alloys with a higher copper content can reach higher R_m values than alloys with 2% Cu. The increase in R_m with variable silicon additions is due to the solution hardening of this alloy. The solid solution of copper in aluminium present in the microstructure, silicon atoms and the Al_2Cu intermetallic phase nucleating at the dislocations and crystallizing at the solution grain boundaries lead to an increase in mechanical properties.

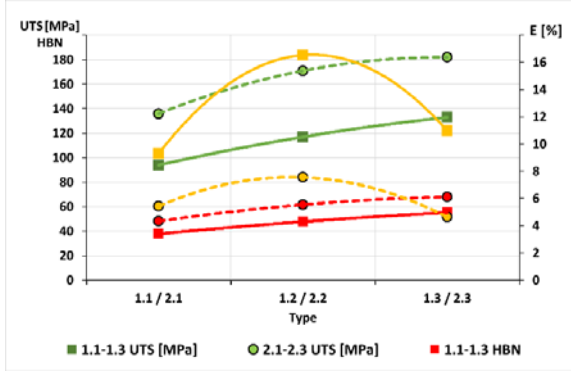

Fig. 10. A comparison of the results of the strength, elongation and hardness testing

Careful analysis of the obtained data shows that silicon addition to the base alloys causes a significant increase in the elongation E, regardless of copper content in the alloy. The elongation was increasing with the increasing addition of silicon. In the remaining cases (samples Nos. 2.1, 2.2 and 2.3), a decrease in elongation was noticed, probably related to the formation of Al_2Cu phases, which contributed to alloy hardening but at the cost of slightly higher brittleness.

Additionally, the samples with 2% Cu content showed a much higher elongation E, i.e. maximum 16.5%, compared to samples with 4% Cu content, which reached the maximum elongation of 7.6%.

Analyzing the results of hardness measurements, it can be concluded that silicon addition has a positive effect on the hardness of individual samples. In all cases, the hardness has increased with respect to the base alloy.

The hardness of the alloy with 2% Cu and 2% Si is 47.8 HB and it increases to 55.2 HB. On the other hand, the hardness of the alloy with 4% Cu and 2% Si is 61.7 HB and it increases to 68.1 HB. The increase in the hardness of the samples is related to the presence of silicon atoms in the crystal structure. The difference in the diameters of Al and Si atoms causes high stresses and elastic deformation of the crystal lattice, which in turn result in the alloy hardening. Additionally, the alloy hardening process can be enhanced by the large precipitates of the Al_2Cu phase.

Microhardness tests carried out on the examined group of alloys allowed determining whether the variable amounts of additives introduced to AlCuSi alloys can cause hardening of these alloys through precipitation of the intermetallic phases, or whether they can also have some impact on the matrix of the examined samples.

The results of microhardness measurements carried out by the Vickers-Hanemann method are presented in Table 6.

The results of microhardness measurements lead to the conclusion that silicon addition has a positive effect on the microhardness of the AlCuSi alloy matrix examined in individual samples of the alloy. In all cases, the microhardness of the aluminium matrix has increased compared to the base alloy.

The microhardness of the alloy with 2% Cu and 2% Si is 55.7 µHV and it increases to 64.8 µHV. On the other hand, the microhardness of the alloy with 4% Cu and 2% Si is 74.6 µHV and it increases to 79.5 µHV.

3.4. Machinability analysis

Machinability was tested by the method which consists in drilling a hole with a constant feed force [6]. The collected results in the form of curves plotted in the hole depth - time system clearly show the machinability of the examined material.

The results of the machinability tests carried out on the examined alloys are shown in Figures 11 - 12.

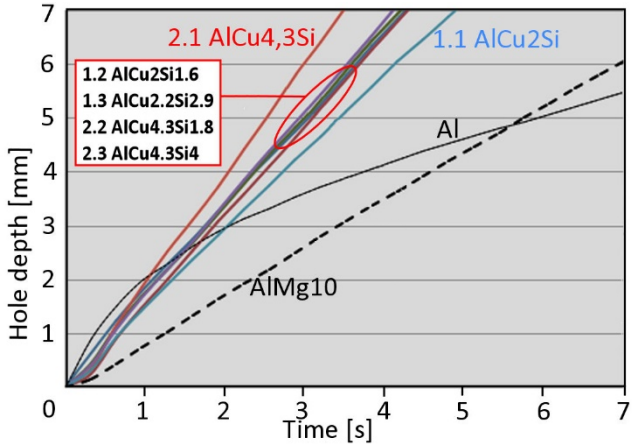

Fig. 11. Averaged machinability results obtained for the examined samples

The method used for the determination and comparison of the machinability of the examined aluminium alloys containing the additions of Cu and Si with samples made from the reference material, i.e. pure aluminium in the form of ingots, and with the AG10 (AlMg10) alloy (described in the literature as machinable and polishable) allows for the following conclusions:

– the shape of the curves on the cutting path - time graph changes, and the changes are related to the cutting process itself. In the initial period of drilling, the drill sinks faster into the material, then chips are formed and their removal increases the cutting resistance and changes the slope of the curves plotted for the examined samples. According to the collected data, the best machinability was obtained in sample No. 2.1 (AlCu4,3Si), while other alloys showed comparable values of the machinability. In pure aluminium ingots, the nature of the cutting was changing in a very clear manner with the elapsing time of testing. In the initial stage, cutting was proceeding very quickly, mainly due to the low hardness of the alloy. Then, chips were formed, which significantly increased the cutting resistance and changed the slope of the curve in the graph illustrating the cutting process,
– the AG10 (AlMg10) alloy used for the comparative analysis was characterized by the machinability slightly inferior to the examined AlCuSi alloys. The AG10 alloy cutting curve indicates the lack of cutting resistance due to chip evacuation nearly throughout the entire drilling range. The appearance of chips generated in the cutting process (Fig. 12) confirms their significant impact on the speed of drilling a hole with a constant feed force.

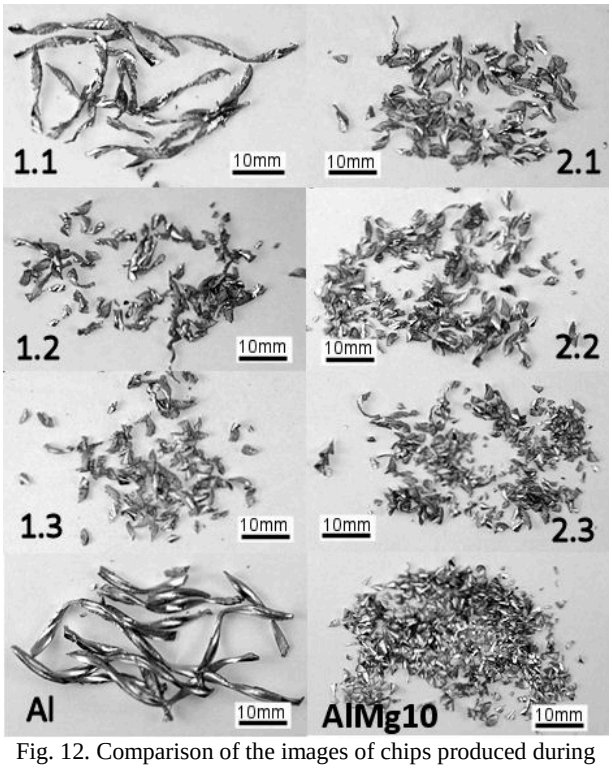

Fig. 12. Comparison of the images of chips produced during machinability testing

4. Conclusions

Testing of primary aluminium alloys with variable additions of copper and silicon has shown a relatively high impact of the additives used.

The results of metallographic tests confirm changes in the grain size, clearly marked by precipitates at the grain boundaries of a solid solution of copper in aluminium. Changes in the number of phase precipitates at the grain boundaries are also observed. Silicon is mainly released in the form of primary precipitates and as an $Al_9Fe_2Si_2$ compound in phases with aluminium and iron in amounts depending on the other constituents. Copper introduced in the form of an AlCu50 master alloy occurs as an Al_2Cu intermetallic phase. Zinc, being in a negligible amount treated as an impurity (up to 0.1%), is transferred into the α solution.

The method of modelling the crystallization process fully reflects what is depicted in the images of the microstructure of the examined alloys, facilitating at the same time an identification of the obtained results. Detailed SEM analysis would confirm the convergence of the obtained results.

Changes in the microstructure are also very clearly visible in the results obtained during testing of the mechanical properties. Owing to the presence of copper and silicon, both strength and hardness increase, while plasticity undergoes changes in the range of 4 to 16%. The alloy with a 4% addition of copper (2.1-2.3) achieves higher tensile strength and hardness. Compared to the alloy with 2% copper content, this is mainly the result of a higher proportional content of the Al_2Cu dispersion precipitates and of the presence of a few primary silicon precipitates, although the latter ones deteriorate the alloy plastic properties.

The hardening of the alloy is also very clearly visible in the results of the machinability tests carried out by the Keep-Bauer method. Both the recorded curves showing the hole depth as a function of time and the images of chips generated during the test indicate an improvement in the wear resistance of the examined aluminium alloys with the additions of copper and silicon. The measurement of machinability gives information not only on the alloy susceptibility to machining by cutting, but also on the wear resistance of the alloys tested.

Increasing the wear resistance of the tested alloys is associated with many stages of casting production, including proper selection of the best chemical composition and of the crystallization and solidification rate. Moreover, the increase in wear resistance depends on the properties of the microstructural constituents, the alloy matrix in particular, and also on the amount and form of the precipitates of the intermetallic phases.

References

[1] Goehler, D.D. (1988). *Proc. of Innovations and Advancements in Aluminum Casting Technology—AFS Special Conf.*, City of Industry, CA (pp. 103–06). American Foundrymen's Society, Des Plaines, Illinois, USA.

[2] Wang, Q.G. (2003). Microstructural effects on the tensile and fracture behavior of aluminum casting alloys A356/357. *Metallurgical and Materials Transactions A: Physical Metallurgy and Materials Science*. 34, 2887–2899. DOI: 10.1007/s11661-003-0189-7.

[3] Farahany, S., Ourdjini, A., Idris, M.H. & Shabestari, S.G., (2013). Computer-aided cooling curve thermal analysis of near eutectic Al-Si-Cu-Fe alloy: Effect of silicon modifier/refiner and solidification conditions on the nucleation and growth of dendrites. *Journal of Thermal Analysis and Calorimetry*. 114, 705–717. DOI: 10.1007/s10973-013-3005-7.

[4] Ghanbari, E., Saatchi, A., Lei, X., & Macdonald, D.D. (2019). Studies on Pitting Corrosion of Al-Cu-Li Alloys Part II: Breakdown Potential and Pit Initiation. *Materials*. 12(11), 1786. DOI: 10.3390/ma12111786.

[5] Ghanbari, E., Saatchi, A., Lei, X., & Macdonald, D.D. (2019). Studies on Pitting Corrosion of Al-Cu-Li Alloys Part III: Passivation Kinetics of AA2098-T851 Based on the Point Defect Model. *Materials*. 12(12), 1912. DOI: 10.3390/ma12121912.

[6] Rzadkosz, S., Zych, J., Piękoś, M., Kozana, J., Garbacz-Klempka, A., Kolczyk, J. & Jamrozowicz, Ł. (2015). Influence of refining treatments on the properties of Al-Si alloys. *Metalurgija*. 54(1), 35–38. http://hrcak.srce.hr/file/187164.

[7] Kozana, J., Piękoś, M., & Garbacz-Klempka, A. (2018) Issues concerning the structure and properties of AlSi7Mg alloys and die castings for the automotive industry. In F. Romankiewicz, R. Romankiewicz, R. Ulewicz (Eds.) *Advanced Manufacturing and Repair Technologies in Vehicle Industry*. (pp.163-191). Zielona Góra (in Polish).

[8] Piękoś, M. & Zych, J. (2019). Investigations of the influence of the zone of chills on the casting made of AlSi7Mg alloy with various wall thicknesses. *Archives of Foundry Engineering*.19(1), 127–132. DOI: 10.24425/afe.2019.127106.

[9] Pysz, S., Maj, M. & Czekaj, E. (2014). High-Strength Aluminium Alloys and Their Use in Foundry Industry of Nickel Superalloys. *Archives of Foundry Engineering*. 14(3). 71–76.

[10] Tupaj, M., Orłowicz, A.W., Mróz, M. Trytek, A. & Markowska, O. (2016). Usable Properties of AlSi7Mg Alloy after Sodium or Strontium Modification. *Archives of Foundry Engineering*. 16(3), 129-132. DOI: 10.1515/afe-2016-0064.

[11] Tupaj, M., Orłowicz, A.W., Trytek, A. & Mróz M. (2019). Improvement of Al-Si Alloy Fatigue Strength by Means of Refining and Modification. *Archives of Foundry Engineering*. 19(4), 61-66. DOI: 10.24425/afe.2019.129631.

[12] Romankiewicz, R. & Romankiewicz, F. (2017). Influence of time on modification effect of silumin AlSi11 with strontium and boron. *Metallurgy and Foundry Engineering*. 43(3), 209-217. DOI: 10.7494/mafe.2017.43.3.209.

[13] Romankiewicz, R. & Romankiewicz, F. (2018). Influence of modification on the refinement of primary silicon crystals in hypereutectic silumin AlSi21CuNi. *Production Engineering Archives*. 19, 30-36. DOI: 10.30657/pea.2018.19.07.

[14] Czekaj, E., Zych, J., Kwak, Z., Garbacz-Klempka, A. (2016) Quality Index of the AlSi7Mg0.3 Aluminium Casting Alloy Depending on the Heat Treatment Parameters. *Archives of Foundry Engineering*. 16(3), 25-28. DOI: 10.1515/afe-2016-0043.

[15] Hirsch, J. & Al-Samman, T. (2013). Superior light metals by texture engineering: Optimized aluminum and magnesium alloys for automotive applications. *Acta Materialia*. 61(3), 818-843. DOI: ISSN 1359-6454.
[16] Hirsch, J. (2014). Recent development in aluminium for automotive applications. Transactions of Nonferrous Metals Society of China. 24(7), 1995-2002. DOI: 10.1016/S1003-6326(14)63305-7.
[17] Tisza, M. & Czinege, I. (2018). Comparative study of the application of steels and aluminium in lightweight production of automotive parts. *International Journal of Lightweight Materials and Manufacture*. 1(4), 229-238. DOI: 10.1016/j.ijlmm.2018.09.001
[18] Starke, E.A., Staley, J.T., (1996). Application of modern aluminum alloys to aircraft. *Progress in Aerospace Sciences*. 32(2), 131–172.
[19] Heinz, A., Haszler, A., Keidel, C., Moldenhauer, S., Benedictus, R. & Miller, W.S. (2000). Recent development in aluminium alloys for aerospace. *Materials Science & Engineering A*. 280(1), 102–107.
[20] Shenglong, Y.S.D. (2005). A glimpse at the development and application of aluminum alloys in aviation industry. *Materials Review*. 2, 022.
[21] Rioja, R. & Liu, J. (2012). The evolution of Al-Li base products for aerospace and space applications. *Metallurgical and Materials Transactions A*. 43, 3325–3337. DOI: 10.1007/s11661-012-1155-z.
[22] Dursun, T. & Soutis, C. (2014). Recent developments in advanced aircraft aluminium alloys. *Materials & Design*. 56, 862–871. DOI: 10.1016/j.matdes.2013.12.002.
[23] Rambabu, P., Eswara Prasad, N., Kutumbarao V.V. & Wanhill, R.J.H. (2017). Aluminium Alloys for Aerospace Applications. In N. Prasad, R. Wanhill (Eds.) *Aerospace Materials and Material Technologies*. (pp.29-52). Indian Institute of Metals Series. Springer, Singapur. DOI: 10.1007/978-981-10-2134-3_2.
[24] Zych, J., Piekło, J., Maj, M., Garbacz-Klempka, A. & Piękoś, M. (2019). Influence of structural discontinuities on fatigue life of 4XXX0-series aluminum alloys. *Archives of Metallurgy and Materials*. 64(2), 765–771. DOI: 10.24425/amm.2019.127611.
[25] Gloria, A., Montanari, R., Richetta, M. & Varone, A. (2019). Alloys for Aeronautic Applications: State of the Art and Perspectives. *Metals*. 9, 662. DOI: 10.3390/met9060662.
[26] Mori, H., Minoda, T., Omura, N., Betsuki, Y., Kojima, Y., Watanabe, Y. & Tanaka, H. (2019). Development of high-strength and high-toughness aluminum alloy. *Journal of Japan Institute of Light Metals*. 69, 9–14. DOI: 10.2464/jilm.69.9.
[27] Górny, M. & Sikora, G. (2015). Effect of titanium addition and cooling rate on primary α(Al) grains and tensile properties of Al-Cu alloy. *Journal of Materials Engineering and Performance*. 24(3), 1150-1156. DOI: 10.1007/s11665-014-1380-2.
[28] Stąpór, S., Górny, M., Kawalec, M. & Gracz, B. (2020) Effect of variable manganese content on microstructure of Al−Cu alloys. *Archives of Metallurgy and Materials*. 65(4), 1377–1383. DOI: 10.24425/amm.2020.133703.
[29] Pan, X.M., Lin, C., Brody, H.D. & Morral J.E. (2005). An assessment of thermodynamic data for the liquid phase in the Al-rich corner of the Al-Cu-Si system and its application to the solidification of a 319 alloy. *Journal of Phase Equilibria and Diffusion*. 26, 225-233. DOI: 10.1007/s11669-005-0109-1.
[30] Ponweiser, N. & Richter, K.W. (2012). New investigation of phase equilibria in the system Al-Cu-Si. *Journal of Alloys and Compounds*. 512, 252-263. DOI: 10.1016/j.jallcom.2011.09.076.
[31] Awe, S.A. (2020). Solidification and microstructural formation of a ternary eutectic Al-Cu-Si cast alloy. *Journal of King Saud University - Engineering Sciences*. DOI: 10.1016/j.jksues.2020.07.004.
[32] Joshi, A., Yogesha, K.K., Kumar, N. & Jayaganthan, R. (2016). Influence of Annealing on Microstructural Evolution, Precipitation Sequence, and Fracture Toughness of Cryorolled Al–Cu–Si Alloy. *Metallogr. Microstruct. Anal.* 5, 540–556. DOI: 10.1007/s13632-016-0313-x
[33] Zhao, G., Ding, C. & Gu, M. (2019). Effects of cooling rate and initial composition on the solidification path and microstructure of Al-Cu-Si alloys. *International Journal of Cast Metals Research*. 32(1), 36-45. DOI: 10.1080/13640461.2018.1507160.
[34] Caceres, C.H., Djurdjevic, M.B., Stockwell, T.J. & Sokolowski, J.H. (1999). The Effect of Cu Content on the Level of Microporosity in Al-Si-Cu-Mg Casting Alloys. *Scripta Materialia*. 40, 631-637.
[35] Djurdjevič, M.B. & Grzinčič, M.A. (2012). The Effect of Major Alloying Elements on the Size of Secondary Dendrite Arm Spacing in the As-Cast Al-Si-Cu Alloys. *Archives of Foundry Engineering*. 12(1), 19-24. DOI: 10.2478/v10266-012-0004-2
[36] Vasconcelos, A.J., Kikuchi, R.H., Barros, A.S., Costa, T.A., Dias, M., Moreira, A.L., Silva, A.P. & da Rocha, O.L. (2016). Interconnection between microstructure and microhardness of directionally solidified binary Al-6wt.%Cu and multicomponent Al-6wt.%Cu-8wt.%Si alloys. *Anais da Academia Brasileira de Ciencias*. 88(2), 1099-1111. DOI: 10.1590/0001-3765201620150172.
[37] Costa, T.A., Moreira, A.L., Moutinho, D.J., Dias, M. Ferreira, I.L., Spinelli, J.E., Rocha, O.L. & Garcia, A. (2015). Growth direction and Si alloying affecting directionally solidified structures of Al–Cu–Si alloys. *Materials Science and Technology*. 31(9), 1103-1112. DOI: 10.1179/1743284714Y.0000000678.
[38] Costa, T.A., Dias, M., Gomes, L.G. Rocha, O.L. & Garcia, A. (2016). Effect of solution time in T6 heat treatment on microstructure and hardness of a directionally solidified Al–Si–Cu alloy. *Journal of Alloys and Compounds*. 683, 485-494. DOI: 10.1016/j.jallcom.2016.05.099.
[39] Ferreira, I.L., Lins, J.F.C., Moutinho, D.J., Gomes, L.G. & Garcia, A. (2010). Numerical and experimental investigation of microporosity formation in a ternary Al–Cu–Si alloy. *Journal of Alloys and Compounds*. 503(1), 31-39. DOI: 10.1016/j.jallcom.2010.04.244.
[40] Wróbel, M. & Burbelko, A. (2015). CALPHAD method - a modern technique for obtaining thermodynamic data (Metoda CALPHAD – nowoczesna technika pozyskiwania

danych termodynamicznych). *Archives of Foundry Engineering*. 14 (si. 3), 79-84 (in Polish).
[41] Wang, C., Huang, F., Lu, Y., Yang, S., Yang, M. & Liu, X. (2013). Experimental Investigation and Thermodynamic Calculation. *Journal of Electronic Materials.* 42(10), 2961-2974. DOI: 10.1007/s11664-013-2695-8.
[42] Andersson, J.O., Helander, T., Höglund, L., Shi, P. & Sundman, B. (2002). Thermo-Calc & DICTRA, computational tools for materials science. *Calphad.* 26(2), 273–312. DOI: 10.1016/S0364-5916(02)00037-8.
[43] Pezda, J. (2008). Effect of modification with strontium on machinability of AK9 silumin. *Archives of Foundry Engineering*. 8 (SI 1), 273-276.